JOC The Journal of Organic Chemistry

pubs.acs.org/joc Article

Sonofragmentation of Organic Molecular Crystals vs Strength of Materials

Hyo Na Kim* and Kenneth S. Suslick*

Cite This: https://dx.doi.org/10.1021/acs.joc.1c00121 Read Online

ACCESS | Metrics & More | Article Recommendations | Supporting Information

ABSTRACT: Mechanochemistry, the interface between the chemical and the mechanical worlds, includes the relationship between the chemical and mechanical properties of solids. In this work, fragmentation of organic molecular crystals during ultrasonic irradiation of slurries has been quantitatively investigated. This has particular relevance to nucleation processes during sonocrystallization, which is increasingly used in the processing and formulation of numerous pharmaceutical agents (PAs). We have discovered that the rates of sonofragmentation are very strongly correlated with the strength of the materials (as measured by Vickers hardness and Young's modulus). This is a mechanochemical extension of the Bell-Evans−Polanyi Principle or Hammond's Postulate: the kinetics (i.e., rates) of solid fracture correlate with thermodynamic properties of solids (e.g., Young's modulus). The mechanism of the particle breakage is consistent with a direct interaction between the shockwaves or localized microjets created by the ultrasound (through acoustic cavitation) and the solid particles in the slurry. Comparisons of the sonofragmentation patterns of ionic and molecular crystals showed that ionic crystals are more sensitive to sonofragmentation than molecular crystals for a given Young's modulus. The rates of sonofragmentation are proposed to correlate with the types and densities of imperfections in the crystals.

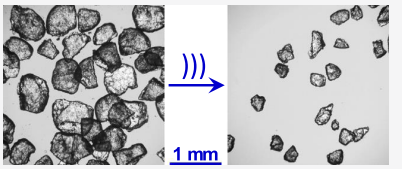

INTRODUCTION[1]

The age-old question of how things break remains an active area of modern research.[2,3] The chemical consequences of fracture and breakage are a major theme in current mechanochemical research.[4−10] Mechanochemical effects change solids physically and chemically and can be induced by a variety of mechanical actions, including trituration, grinding, milling, and ultrasound.[11,12] When mechanical actions are applied to molecular solids, the fracture can also occur, but our fundamental understanding of the nature of the breakage of organic molecular crystals as a function of their chemical and mechanical properties remains limited. This is not surprising, given that molecular crystals are not generally structural materials (such as ceramics, metals, or polymers) and consequently have not been subjected to an extensive examination of their mechanical properties. Specifically, the fragmentation of solid particles in liquid slurries subjected to mechanical action (e.g., ultrasonic irradiation) has received relatively little attention.[13−18] Sonofragmentation of pharmaceutical agents (PAs, or active pharmaceutical ingredients, APIs), however, plays a critical role in sonocrystallization, which has proved extremely efficacious in PA processing, formulation, and crystallization.[16,17,19−22] To examine and control the fundamental events during sonofragmentation, we examine here fundamental experiments on the fragmentation of organic molecular crystals during sonication of slurries and compare the kinetics of the resulting fragmentation with the strength of the materials.

The effects of ultrasound on slurries of malleable metal powders have shown surface modifications in the morphology, agglomeration, and removal of passivating coatings with dramatic increases in surface chemical reactivity.[23−29] In contrast, ultrasonic treatment of slurries of brittle molecular and ionic crystals leads to rapid fracture and is important for our understanding of sonocrystallization, a process of increasing importance to the pharmaceutical industry.[17,18,21,30−33]

When a liquid is irradiated with high-intensity ultrasound, acoustic cavitation (the formation, growth, and implosive collapse of bubbles) occurs.[23,34,35] During the bubble collapse, intense localized heating occurs, and shockwaves emanate from the bubble rebound. Hot spots are created with extreme local temperatures (~5000 K) and pressures (~1000 atm), but with extraordinary heating/cooling rates (>10^{10} K s^{-1}).[36,37] The propagating shockwave velocity and pressure can be as high as ~4000 m/s and 1 GPa, respectively,[38] and, therefore, possess enough energy to change materials both physically and chemically. In addition, at extended surfaces (greater than ~200 μm at 20 kHz), cavitation collapse is asymmetric and can generate a high-speed microjet directed at the surface.[23,34,35]

When ultrasound is applied to a slurry of molecular or ionic crystals, sonofragmentation of the crystals occurs, and we have previously shown that the fragmentation mechanism results from a direct interaction between crystals and cavitation-

Special Issue: Enabling Techniques for Organic Synthesis

Received: January 15, 2021

https://dx.doi.org/10.1021/acs.joc.1c00121
J. Org. Chem. XXXX, XXX, XXX−XXX

induced shockwaves or microjets and not from interparticle collisions or impaction.[15,16] This is an important part of the sonocrystallization process.[16−22,30,32,39] By fracturing existing crystals, new secondary nucleation sites are created,[19,40−43] and overgrown crystals are reduced in size.[15,16] Sonocrystallization thus provides control over crystallization (both in time and space) and produces smaller crystals more rapidly and with narrower size distributions than traditional crystallization methods: all particularly desirable traits for the processing of pharmaceutical agents.

RESULTS AND DISCUSSION

The effects of various control variables (e.g., acoustic power density, frequency, solvent, etc.) on sonofragmentation of particles have been reported.[16,20,22,44−47] The relationship, however, between the physical properties of molecular crystals (e.g., the strength of materials) and ease of sonofragmentation has not previously been reported. We have sonicated slurries of ten different molecular crystals, specifically of six pharmaceutically relevant hydrogen-bonding molecules (HBM) and of four polycyclic aromatic hydrocarbons (PAH). The Vickers hardness (H_v) and Young's modulus (a measure of the stiffness of a material, E)[48−50] were determined for each of these crystals and the relationship between the strength of these crystals and ease of sonofragmentation compared for both classes of molecular crystals and for ionic crystals as well.

As described in detail in the Experimental Procedures section below, all sonications were done with 0.15 wt % slurries of the crystals using a 20 kHz titanium horn operated at 10 W/cm^2. The steady state temperatures during sonication were 25 °C using a 20% duty cycle to minimize temperature variation. The HBM crystals were selected to span a range of hardnesses, specifically we examined sucrose, lactose, acetaminophen (i.e., paracetamol, a common analgesic), phenacetin (analgesic), sulfadimethoxine (a sulfonamide antibiotic), and hexamethylenetetramine (i.e., hexamine, a common reagent and preservative). The PAH crystals were of anthracene, pyrene, chrysene, and 9,10-diphenylanthracene.

The rate and extent of sonofragmentation were determined by direct observation using optical microscopy (Figure 1 and Figures S1 and S2) from aliquots taken for analysis. Size distributions were measured using the longest dimension (i.e., length) of particles from each aliquot using approximately 200 particles with Image-J software. The rate of fragmentation for the molecular crystals is shown in Figure 2. The data revealed an exponential reduction in particle size as a function of sonication time.

The effects of initial crystal size on sonofragmentation were also evaluated. Sucrose was chosen partly due to its low cost and partly due to its high hardness and stiffness. Seven different particle sizes of sucrose were prepared by sieving in a sonic sifter (Figure S3) and, for the smallest particles, grinding prior to sieving. Figures S4 and S5 show the morphologies and crystal sizes of particles in each sucrose group. The mean crystal sizes were determined by direct measurement and counting of the longest dimension (i.e., length) of particles through optical and SEM micrographs. The initial mean lengths of crystals in size groups 1 through 7 were 1054 μm, 680 μm, 310 μm, 140 μm, 68 μm, 14 μm, and 0.56 μm, respectively (Figure S6).

For slurries of particles larger than ~20 μm in initial crystal size, no effects of initial size were observed on the rates of fragmentation of molecular crystals (Figure 3). Sonofragmentation, however, was suppressed for initial crystals smaller than about 10 μm (Figure 3, group 6 after 240 s sonication and group 7). Indeed, no fragmentation at all was observed with slurries of crystals whose initial mean size was 0.56 μm (group 7). When the molecular crystal slurries are irradiated by ultrasound, the crystals were broken by direct interaction with shockwaves or microjets created by acoustic cavitation.[15,16] Forming microjets during cavitation, however, requires a rather large particle

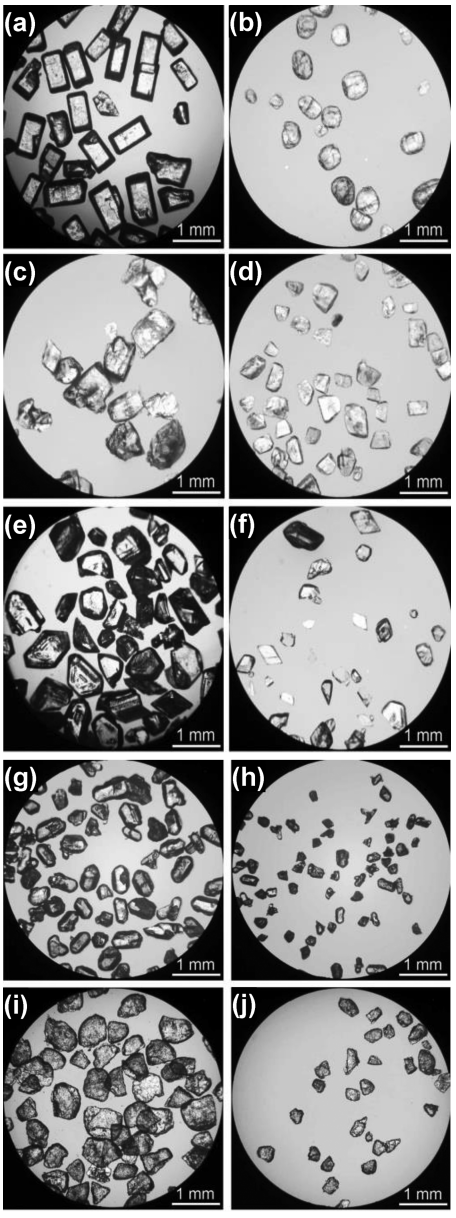

Figure 1. Optical micrographs of representative molecular crystals before and after sonication showing rapid sonofragmentation. Hydrogen-bonding crystals: (a) Sucrose before sonication and (b) after sonication 480 s, (c) acetaminophen before sonication and (d) after sonication 380 s, and (e) hexamethylenetetramine before sonication and (f) after sonication for 210 s. Each slurry of hydrogen-bonding molecular crystals contained 0.15 wt % of molecular crystals in dodecane and was sonicated by using a titanium horn (10 W/cm^2 and 20 kHz). PAH crystals: (g) 9,10-diphenylanthracene before sonication and (h) after sonication for 300 s and (i) anthracene before sonication and (j) after sonication for 270 s. Each slurry of PAH crystals contained 0.15 wt % of PAH crystals in DI water and was sonicated by using a titanium horn (10 W/cm^2 and 20 kHz). Figure S1 and S2 show further examples.

https://dx.doi.org/10.1021/acs.joc.1c00121
J. Org. Chem. XXXX, XXX, XXX−XXX

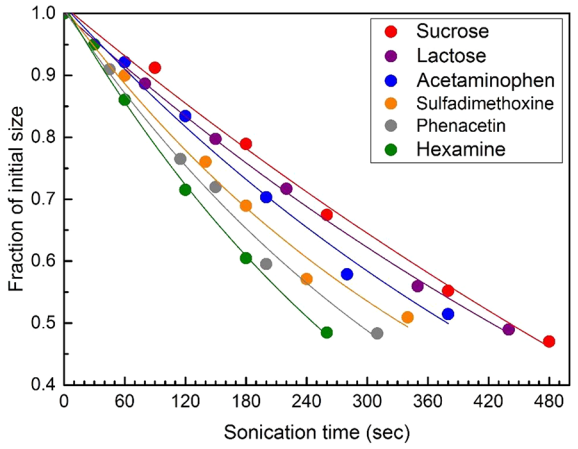

Figure 2. Kinetics of sonofragmentation. The size of crystals normalized to the initial crystal size is shown versus sonication time for various molecular crystals. Slurries containing 0.15 wt % of these hydrogen-bonding molecular crystals in dodecane were sonicated using a titanium horn (10 W/cm^2 at 20 kHz). Solid lines are exponential fits to the data. Experiments were run in quadruplicate, and relative standard deviations of the particle length determinations are <4%.

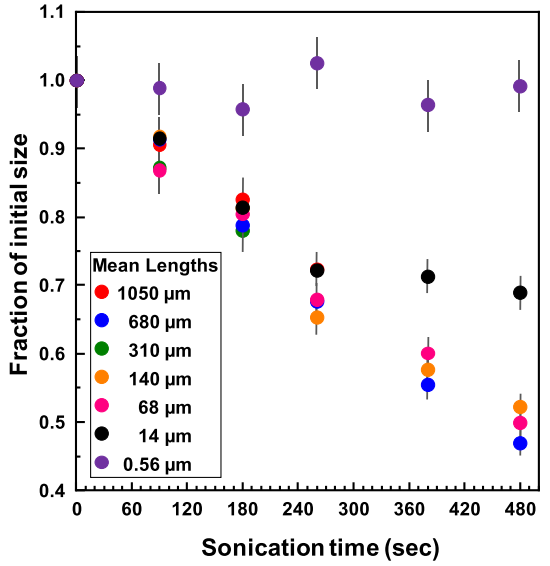

Figure 3. Effect of initial crystal size on the fragmentation of sucrose crystals. For each size group, a slurry containing 0.15 wt % sucrose in 10 mL of dodecane was sonicated using a titanium horn (10 W/cm^2 and 20 kHz). The longest dimensions of the crystals for each size group are given in the legend. Relative standard deviations for each data point are <7%.

(greater than ~200 μm for 20 kHz) to cause bubble distortion during collapse;[23,34,35] the fracture of smaller particles (down to 20 μm) here suggests that microjets are likely to be only a minor contributor to particle fracture. Under the sonication of slurries, crystals keep breaking until they are too small to be fragmented by shockwaves passing through the slurry, and this has been well-fit by simple population models.[51] When the crystals reach a critical small size, however, the shock-induced stress over the length of the crystal that cavitation creates no longer exceeds the tensile strength of the crystal. The minimum size for sonofragmentation will depend on the frequency and intensity of the irradiated ultrasound. In these experiments, with ultrasonic irradiation at 20 kHz and 10 W/cm^2, molecular crystals smaller than roughly 10 μm in length are no longer prone to sonofragmentation.

The Vickers hardness (H_v) and Young's modulus (E) values for all crystals were determined by standard methods,[48−50] using a Vickers indenter and an Agilent nanoindenter, respectively (Table 1). The ranges of Vickers hardness and Young's modulus

Table 1. Vickers Hardness (H_v) and Young's modulus (E) vs the Sonofragmentation $\tau_{1/2}$ (i.e., Length of Sonication Time Necessary to Halve the Initial Crystal Size) of Molecular Crystals

molecular crystals[a]	$\tau_{1/2}$ (sec)[b]	H_v (GPa)[c]	E (GPa)[c]	initial crystal size (μm)[d]
sucrose	480	0.64	32.3	678
lactose	440	0.54	24.1	664
acetaminophen	380	0.36	18.1	561
sulfadimethoxine	340	0.24	N/A	442
phenacetin	310	0.172	N/A	1162
chrysene	310	0.180	13.6	677
9,10-diphenylanthracene	300	0.210	12.8	793
pyrene	270	0.071	7.6	748
anthracene	270	0.052	9.4	925
hexamethylenetetramine	260	0.133	9.0	507

[a]Hydrogen-bonding molecular crystals (bold) and polycyclic aromatics (italic). [b]Relative standard deviations are <4%. [c]Relative standard deviations are <5%. [d]Longest dimension.

of the HBM crystals partially overlapped with those of the PAH crystals were used in this project. For each of the molecular crystals, H_v and E were compared to $\tau_{1/2}$ (the length of sonication required to reduce the crystal size distribution to half of the initial size), as shown in Table 1.

The relationship between sonofragmentation kinetics and either the Vickers hardness (H_v) or Young's modulus (E) is plotted in Figure 4. There is a tight linear relationship between H_v and $\tau_{1/2}$ and between E and $\tau_{1/2}$. Interestingly, the HBM and PAH crystals are colinear. These results are consistent with similar correlations between the mechanical properties of various molecular crystals and final size reduction by mechanical milling or particle impaction during jet-milling.[52−55]

Ionic, hydrogen-bonding molecular, and polycyclic aromatic hydrocarbon crystals are held together by various types of intermolecular and interatomic interactions.[56] In ionic crystals, the major forces are ion-to-ion electrostatic attractions, which are strong long-range interactions. In contrast, in molecular crystals, that lattice is held together by weak intermolecular forces, primarily polarization (e.g., dipole−dipole) interactions, and van der Waals (dispersion) forces and, in some cases, hydrogen-bonding between molecules. For molecular solids, the local length scales of these intermolecular forces are relatively short, especially hydrogen bonding.[57−60] PAH crystals generally have the weakest intermolecular interactions since intermolecular hydrogen bonds generally give greater stability to HBM crystals and ion−ion electrostatic interactions are the strongest. Thus, the strength of intermolecular interactions in the materials evaluated here compared with our earlier work on ionic crystals[15] is generally ionic crystals > HBM crystals > PAH crystals, which of course follows the crystal melting points for similar molecular weight components.

Intuitively, one might have expected that there would therefore be a universal correlation between rates of fragmentation and the strength of intermolecular interactions

https://dx.doi.org/10.1021/acs.joc.1c00121
J. Org. Chem. XXXX, XXX, XXX−XXX

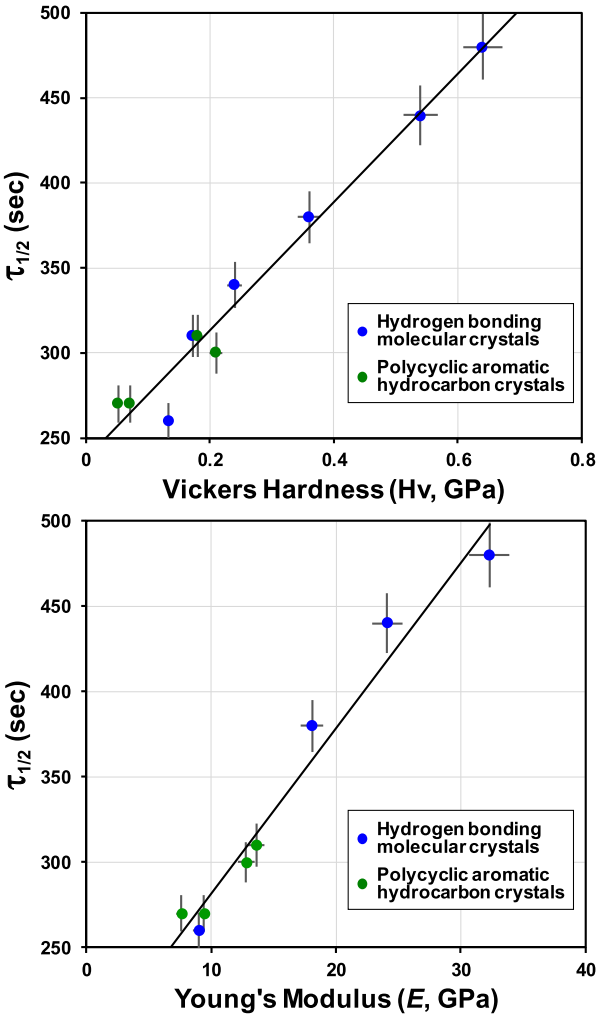

Figure 4. Relationship between rate of sonofragmentation of molecular crystals and either Vickers hardness or Young's modulus. (a) Vickers hardness (H_v) vs log $\tau_{1/2}$ (i.e., the time necessary to halve the initial crystal size) and (b) Young's modulus (E) vs log $\tau_{1/2}$. Blue markers are hydrogen-bonding molecular crystals, and green markers are polycyclic aromatic hydrocarbon crystals. A linear fit to the data is shown.

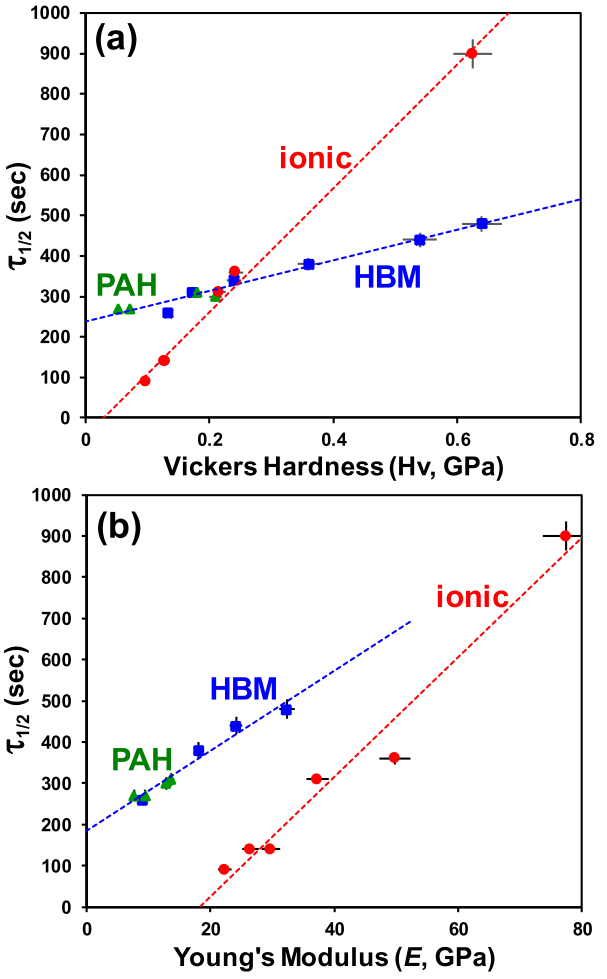

Figure 5. Comparison of the relationships between (a) Vickers hardness (H_v) and the time necessary to halve the initial crystal size ($\tau_{1/2}$) of ionic, hydrogen-bonding molecular (HBM), and PAH crystals and (b) Young's modulus (E) and the time necessary to halve the initial crystal size ($\tau_{1/2}$) of ionic, hydrogen-bonding molecular, and PAH crystals. The dashed lines are linear fits. Relative standard deviations are <5%. The ionic solids used here (listed from lowest E or H_v to highest) are NaF, LiCl, NaCl, NaBr, KCl, and KBr.[15]

within the crystals. As we will see, however, the nature of fragmentation is more complex. For either ionic crystals or molecular crystals, we do indeed observe excellent linear relationships between the observed rate of fragmentation with either the measured hardness or stiffness of the crystals, as shown in Figure 5. It is rather striking, however, that the ionic crystals and the molecular crystals are not even approximately colinear in these plots. Sonofragmentation of ionic crystals showed a significantly higher sensitivity to changes in hardness (H_v) or stiffness (E) among the materials. Somewhat counter-intuitive to the chemist, the strength of these materials as measured by Young's Modulus (E) or Vickers Hardness (H_v) is not directly related to the nature of the intermolecular forces within the solids (i.e., stronger electrostatic forces for ionic solids vs weaker dipolar and van der Waals forces for molecular solids). As seen in Figure 5, there are both very hard and very soft ionic solids that overlap the range of the molecular solids examined here.

In a sense, breakage of solids is a nucleated process: imperfections in the structure of the solid with long-range consequences (e.g., planar or bulk imperfections, especially on surfaces, including grain boundary mismatches, edge or screw dislocations, microcracks, and inclusions, etc.) are likely to make fracture and fragmentation facile.[61−65] In contrast, a single, localized defect (e.g., Frenkel or Schottky point defects) will not make a crystal easy to break. Crystal breakage initiates from pre-existing imperfections in the particle, particularly surface imperfections that can cause stress concentrations from which crack propagation can proceed until cleavage is attained. The length scale of an order may affect the propagation of cracks and thereby affect the sensitivity of sonofragmentation to a material's hardness. In addition to the types of imperfections present, the initial density of imperfections and their location will have a substantial impact on susceptibility to fragmentation.[61−64] Thus, the combined effect of the type and density of imperfections will determine the sensitivity of any particular crystal to sonofragmentation. It is truly remarkable, however, that within the same class of crystals (i.e., ionic vs molecular) such linearity is observed between the kinetics of fragmentation and the mechanical properties of hardness or stiffness. The greater sensitivity of ionic crystals to changes in H_v or E probably reflects differences in the types of defects and imperfections found in

https://dx.doi.org/10.1021/acs.joc.1c00121
J. Org. Chem. XXXX, XXX, XXX−XXX

ionic crystals compared to molecular crystals or the ease at which microjets may damage their respective surfaces.

Because fragmentation of crystals is a nucleated process, sonofragmentation is not inherently related to the solids' hardness or bulk modulus. Nonetheless, intuitively one expects that the rate at which defects and imperfections are generated in solid particles during strain or impact ought to correlate with the strength of materials. This is a mechanochemical extension of the Bell-Evans−Polanyi Principle or of Hammond's Postulate: kinetics correlate with thermodynamics.[66,67]

Indeed, prior reports have established empirically that fracture toughness and fracture strength of glasses (both silica and metallic) are often proportional to Young's modulus.[68,69] There are also similar results for various minerals, and harder minerals require more energy to be broken.[70] None of these studies, however, examined the kinetics of particle breakage. As we have now observed for both ionic and molecular crystals, the rate of breakage correlates strongly with both Young's modulus and the Vickers hardness of these crystals: i.e., the kinetics of sonofragmentation ($\tau_{1/2}$) correlates with thermodynamic and mechanical properties (H_v and E).

The effects of crystal anisotropy or asymmetry (both in bulk morphology and in the crystallographic space group) have not been addressed in this study, and so remain an interesting matter for future work. The crystals examined in these studies are generally relatively cubic (i.e., not needles or sheets), and we, therefore, did not observe significant differences in the kinetics of fracture. Similarly, we were not able to measure E or H as a function of crystallographic facets, although for molecular crystals, this dependence is likely to be relatively small since the intermolecular interactions within the crystal are usually not especially anisotropic and are generally relatively short-range.

CONCLUSIONS

Organic molecular crystals were fragmented by ultrasonic irradiation of slurries; both hydrogen-bonding and polycyclic aromatic molecular crystals were examined. The particle size of the molecular crystals decreased exponentially during sonication. For very small molecular crystals (<15 μm), little or no sonofragmentation occurred since the negative pressure generated from the propagating shockwaves created by acoustic cavitation cannot exceed tensile strength over the diminished length of the crystal. There was an excellent correlation between the rate of fragmentation and the materials' thermodynamic and mechanical properties (i.e., the strength of the materials as indicated by Vickers hardness or Young's modulus). The sonofragmentation of ionic crystals was more sensitive to changes in the strength of the materials compared to molecular crystals.

EXPERIMENTAL PROCEDURES

Materials. Lactose, acetaminophen, hexamethylenetetramine, chrysene, 9,10-diphenylanthracene, pyrene, anthracene, and dodecane were purchased from Sigma-Aldrich. Sucrose was purchase from Fisher Scientific. All chemicals were used as received, unless otherwise indicated. Sulfadimethoxine and phenacetin (Sigma-Aldrich) were recrystallized in nanopure water (i.e., water deionized to >18 MΩ cm resistance, scrubbed for organics, and passed through a 0.45 μm filter with a Barnstead NANOpure ultrapure water purification system).

Sonofragmentation Experimental Setup. For the HBM crystals, slurries were prepared from 10 mL of dodecane added to 15 mg of the crystals. The slurry was thermally equilibrated at 18 °C for 5 min in a temperature-controlled water bath (Isotemp 1006S). This mixture was sonicated with an exponential ultrasonic horn (Sonics and Materials VCX-750, 20 kHz, 1 cm^2 Titanium tip, 10 W/cm^2) for various times. All sonication experiments were performed using a duty cycle of 2 s on and 8 s off pulse cycle to reduce temperature variation. For all cases, steady state temperatures during sonication were 25 °C. Sonication times are reported as the total time exposed to ultrasound. For the sonofragmentation experiments of polycyclic aromatic hydrocarbon (PAH) crystals, slurries were made by adding 10 mL of DI water to 15 mg of PAH crystals. Other experimental conditions and processes were same as those of sonofragmentation experiments of the HBM crystals.

All kinetic runs were done in quadruplicate. The particle size data were obtained from micrographs as detailed below as a function of the length of sonication. Kinetic studies were run until the particle size (measured largest dimension) was decreased to approximately half of the initial size (Figure 2). All data were fit well by a simple exponential fit, and an effective sonofragmentation $\tau_{1/2}$ (i.e., length of sonication time necessary to halve the initial crystal size) was obtained for each sonofragmentation experiment. Reproducibility of the $\tau_{1/2}$ values was excellent, with the relative standard deviation within 4% (Table 1).

Sample Preparation of Sucrose Having Different Crystal Sizes. In order to check the effect of initial crystal size, a sonic sifter (Advantech Manufacturing, Berlin, WI) was used with various sieves (mesh opening sizes 45, 75, 106, 250, 500, and 1000 μm) to separate batches of sucrose based on their size. The sonic sifter was used for 5 min. Crystals that were not sieved by the sifter were removed. The sieved crystals were collected and sieved again with the same intensity and time. This process was done total 4 times for each size group of sucrose. For the crystals passing the sieve with a mesh opening size of 45 μm, vacuum filtration was performed with filter paper (pore size 1.2 μm), and the filtered crystals were taken for group 6.

For the group of the smallest size of sucrose (group 7), sucrose was first ground by mortar and pestle and then sieved with a mesh opening size of 45 μm. Crystals smaller than 45 μm then collected and dispersed into dodecane. Finally, for size group 7, the sucrose−dodecane slurry was sonicated with an ultrasonic horn (20 kHz and 40 W/cm^2) for an hour; after the sonication, sucrose particles were collected by centrifuge and dried in a vacuum oven at room temperature overnight.

Image, Particle Size, and Materials Characterization. An aliquot of the sonicated slurry was removed using a disposable pipet for analysis by optical microscopy (Zeiss Axioskop optical/fluorescence microscope). The micrographs were captures using a Cannon PC1015 digital camera mounted to the microscope. Scanning electron microscopy was performed with a JEOL 7000F Analytical SEM.

Crystal size analysis with optical microscopic or SEM images was performed using Image-J software (National Institutes of Health, Bethesda, MD, USA). The longest dimension (i.e., length) of approximately 200 well-isolated particles were measured for each experiment, as shown in Figure S6. Data fitting was performed using OriginPro 8.5 software (OriginLab, Northampton, MA, USA).

Vickers hardness and Young's modulus of crystals were measured by Leitz Wetzlar GMBH and Agilent G200 Nanoindenter, respectively. Quintuplicate measurements of H_v and E were made for each of the molecular solids, and relative standard deviations were <5%.

ASSOCIATED CONTENT

Supporting Information

The Supporting Information is available free of charge at https://pubs.acs.org/doi/10.1021/acs.joc.1c00121.

Optical and SEM micrographs, sieving methodology, and size distributions (PDF)

AUTHOR INFORMATION

Corresponding Authors

Hyo Na Kim − *Department of Chemistry, Gachon University, Seongnam-si, Gyeonggi-do 13120, Republic of Korea*; Email: hyonakim@gachon.ac.kr

https://dx.doi.org/10.1021/acs.joc.1c00121
J. Org. Chem. XXXX, XXX, XXX−XXX

Kenneth S. Suslick − *Department of Chemistry, University of Illinois at Urbana−Champaign, Urbana, Illinois 60801, United States;* orcid.org/0000-0001-5422-0701; Email: ksuslick@illinois.edu

Complete contact information is available at: https://pubs.acs.org/10.1021/acs.joc.1c00121

Notes

The authors declare no competing financial interest.

REFERENCES

(1) Reproduced in part from the Ph.D. dissertation of Hyo Na Kim, which is accessible using the following link: https://www.ideals.illinois.edu/handle/2142/98211.
(2) Hill, H. The Paradox of Fiber Failure. *Phys. Today* **2020**, *73* (7), 20200702a.
(3) Fontana, J.; Palffy-Muhoray, P. St. Petersburg Paradox and Failure Probability. *Phys. Rev. Lett.* **2020**, *124*, 245501.
(4) Beyer, M. K.; Clausen-Schaumann, H. Mechanochemistry: the mechanical activation of covalent bonds. *Chem. Rev.* **2005**, *105*, 2921−2948.
(5) Jones, W.; Eddleston, M. D. Introductory lecture: mechanochemistry, a versatile synthesis strategy for new materials. *Faraday Discuss.* **2014**, *170*, 9−34.
(6) Caruso, M. M.; Davis, D. A.; Shen, Q.; Odom, S. A.; Sottos, N. R.; White, S. R.; Moore, J. S. Mechanically-Induced Chemical Changes in Polymeric Materials. *Chem. Rev.* **2009**, *109*, 5755−5798.
(7) Friščić, T.; James, S. L.; Boldyreva, E. V.; Bolm, C.; Jones, W.; Mack, J.; Steed, J. W.; Suslick, K. S. Highlights from Faraday discussion 170: Challenges and opportunities of modern mechanochemistry, Montreal, Canada, 2014. *Chem. Commun.* **2015**, *51*, 6248−6256.
(8) James, S. L.; Adams, C. J.; Bolm, C.; Braga, D.; Collier, P.; Friscic, T.; Grepioni, F.; Harris, K. D. M.; Hyett, G.; Jones, W.; Krebs, A.; Mack, J.; Maini, L.; Orpen, A. G.; Parkin, I. P.; Shearouse, W. C.; Steed, J. W.; Waddell, D. C. Mechanochemistry: opportunities for new and cleaner synthesis. *Chem. Soc. Rev.* **2012**, *41*, 413−447.
(9) Ralphs, K.; Hardacre, C.; James, S. L. Application of heterogeneous catalysts prepared by mechanochemical synthesis. *Chem. Soc. Rev.* **2013**, *42*, 7701−7718.
(10) Lee, B.; Niu, Z.; Wang, J.; Slebodnick, C.; Craig, S. L. Relative Mechanical Strengths of Weak Bonds in Sonochemical Polymer Mechanochemistry. *J. Am. Chem. Soc.* **2015**, *137*, 10826−10832.
(11) Cravotto, G.; Gaudino, E. C.; Cintas, P. On the mechanochemical activation by ultrasound. *Chem. Soc. Rev.* **2013**, *42*, 7521−7534.
(12) Suslick, K. S. Mechanochemistry and sonochemistry: concluding remarks. *Faraday Discuss.* **2014**, *170*, 411−422.
(13) Guo, Z.; Jones, A. G.; Li, N.; Germana, S. High-speed observation of the effects of ultrasound on liquid mixing and agglomerated crystal breakage processes. *Powder Technol.* **2007**, *171*, 146−153.
(14) Wagterveld, R. M.; Boels, L.; Mayer, M. J.; Witkamp, G. J. Visualization of acoustic cavitation effects on suspended calcite crystals. *Ultrason. Sonochem.* **2011**, *18*, 216−225.
(15) Kim, H. N.; Suslick, K. S. Sonofragmentation of Ionic Crystals. *Chem. - Eur. J.* **2017**, *23*, 2778−2782.
(16) Zeiger, B. W.; Suslick, K. S. Sonofragmentation of Molecular Crystals. *J. Am. Chem. Soc.* **2011**, *133*, 14530−14533.
(17) Sander, J. R. G.; Zeiger, B. W.; Suslick, K. S. Sonocrystallization and sonofragmentation. *Ultrason. Sonochem.* **2014**, *21*, 1908−1915.
(18) Kim, H.; Suslick, K. The effects of ultrasound on crystals: Sonocrystallization and sonofragmentation. *Crystals* **2018**, *8*, 280.
(19) Zhang, Z.; Sun, D.-W.; Zhu, Z.; Cheng, L. Enhancement of crystallization processes by power ultrasound: current state-of-the-art and research advances. *Compr. Rev. Food Sci. Food Saf.* **2015**, *14*, 303−316.
(20) Narducci, O.; Jones, A. G.; Kougoulos, E. An assessment of the use of ultrasound in the particle engineering of micrometer-scale adipic acid crystals. *Cryst. Growth Des.* **2011**, *11*, 1742−1749.
(21) de los Santos Castillo-Peinado, L.; Luque de Castro, M. D. The role of ultrasound in pharmaceutical production: sonocrystallization. *J. Pharm. Pharmacol.* **2016**, *68*, 1249−1267.
(22) Belkacem, N.; Salem, M. A. S.; AlKhatib, H. S. Effect of ultrasound on the physico-chemical properties of poorly soluble drugs: Antisolvent sonocrystallization of ketoprofen. *Powder Technol.* **2015**, *285*, 16−24.
(23) Suslick, K. S. Sonochemistry. *Science* **1990**, *247*, 1439−1445.
(24) Suslick, K. S. Applications of ultrasound to materials chemistry. *MRS Bull.* **1995**, *20*, 29−34.
(25) Bang, J. H.; Suslick, K. S. Applications of ultrasound to the synthesis of nanostructured materials. *Adv. Mater.* **2010**, *22*, 1039−1059.
(26) Xu, H.; Zeiger, B. W.; Suslick, K. S. Sonochemical synthesis of nanomaterials. *Chem. Soc. Rev.* **2013**, *42*, 2555−2567.
(27) Prozorov, T.; Prozorov, R.; Suslick, K. S. High velocity interparticle collisions driven by ultrasound. *J. Am. Chem. Soc.* **2004**, *126*, 13890−13891.
(28) Doktycz, S. J.; Suslick, K. S. Interparticle collisions driven by ultrasound. *Science* **1990**, *247*, 1067−1069.
(29) Suslick, K. S.; Price, G. J. Applications of ultrasound to materials chemistry. *Annu. Rev. Mater. Sci.* **1999**, *29*, 295−326.
(30) Ruecroft, G.; Hipkiss, D.; Ly, T.; Maxted, N.; Cains, P. W. Sonocrystallization: the use of ultrasound for improved industrial crystallization. *Org. Process Res. Dev.* **2005**, *9*, 923−932.
(31) de Castro, M. D. L.; Priego-Capote, F. Ultrasound-assisted crystallization (sonocrystallization). *Ultrason. Sonochem.* **2007**, *14*, 717−724.
(32) Jordens, J.; Gielen, B.; Xiouras, C.; Hussain, M. N.; Stefanidis, G. D.; Thomassen, L. C. J.; Braeken, L.; Van Gerven, T. Sonocrystallisation: Observations, theories and guidelines. *Chem. Eng. Process.* **2019**, *139*, 130−154.
(33) Jiang, M.; Braatz, R. D. Designs of continuous-flow pharmaceutical crystallizers: developments and practice. *CrystEngComm* **2019**, *21*, 3534−3551.
(34) Leighton, T. *The Acoustic Bubble*; Academic Press, 2012.
(35) Brennen, C. E. *Cavitation and Bubble Dynamics*; Cambridge University Press, 2014.
(36) Suslick, K. S.; Flannigan, D. J. Inside a collapsing bubble: Sonoluminescence and the conditions during cavitation. *Annu. Rev. Phys. Chem.* **2008**, *59*, 659−683.
(37) Suslick, K. S.; Eddingsaas, N. C.; Flannigan, D. J.; Hopkins, S. D.; Xu, H. The Chemical History of a Bubble. *Acc. Chem. Res.* **2018**, *51*, 2169−2178.
(38) Pecha, R.; Gompf, B. Microimplosions: Cavitation collapse and shock wave emission on a nanosecond time scale. *Phys. Rev. Lett.* **2000**, *84*, 1328−1330.
(39) Cains, P. W.; Martin, P. D.; Price, C. J. The use of ultrasound in industrial chemical synthesis and crystallization. 1. Applications to synthetic chemistry. *Org. Process Res. Dev.* **1998**, *2*, 34−48.
(40) Agrawal, S. G.; Paterson, A. H. J. Secondary nucleation: mechanisms and models. *Chem. Eng. Commun.* **2015**, *202*, 698−706.
(41) Chow, R.; Blindt, R.; Chivers, R.; Povey, M. The sonocrystallisation of ice in sucrose solutions: primary and secondary nucleation. *Ultrasonics* **2003**, *41*, 595−604.
(42) Chow, R.; Blindt, R.; Kamp, A.; Grocutt, P.; Chivers, R. The microscopic visualisation of the sonocrystallisation of ice using a novel ultrasonic cold stage. *Ultrason. Sonochem.* **2004**, *11*, 245−250.
(43) Chow, R.; Blindt, R.; Chivers, R.; Povey, M. A study on the primary and secondary nucleation of ice by power ultrasound. *Ultrasonics* **2005**, *43*, 227−230.
(44) Raman, V.; Abbas, A. Experimental investigations on ultrasound mediated particle breakage. *Ultrason. Sonochem.* **2008**, *15*, 55−64.
(45) Jordens, J.; Appermont, T.; Gielen, B.; Van Gerven, T.; Braeken, L. Sonofragmentation: effect of ultrasound frequency and power on particle breakage. *Cryst. Growth Des.* **2016**, *16*, 6167−6177.
(46) Alexandre, M.; Perez, E.; Lacabanne, C.; Dantras, E.; Franceschi, S.; Coudeyre, D.; Garrigues, J.-C. Formulation of aqueous dispersions of PEKK by a quantitative structure property relationship approach and

application to thermoplastic sizing on carbon fibers. *Adv. Mater. (N. Y., NY, U. S.)* **2018**, *7*, 118.
(47) Nimmy, E.; Wilson, P. Investigations on sonofragmentation of hydroxyapatite crystals as a function of strontium incorporation. *Ultrason. Sonochem.* **2019**, *50*, 188−199.
(48) Ichikawa, J.; Imagawa, K.; Kaneniwa, N. The effect of crystal hardness on compaction propensity. *Chem. Pharm. Bull.* **1988**, *36*, 2699−2702.
(49) Duncanhewitt, W. C.; Weatherly, G. C. Evaluationg the hardness, Young modulus and fracture-toughness of some pharmaceutical crystals using microindentation techniques. *J. Mater. Sci. Lett.* **1989**, *8*, 1350−1352.
(50) Perkins, M.; Ebbens, S. J.; Hayes, S.; Roberts, C. J.; Madden, C. E.; Luk, S. Y.; Patel, N. Elastic modulus measurements from individual lactose particles using atomic force microscopy. *Int. J. Pharm.* **2007**, *332*, 168−175.
(51) Rasche, M. L.; Zeiger, B. W.; Suslick, K. S.; Braatz, R. D. Mathematical modelling of the evolution of the particle size distribution during ultrasound-induced breakage of aspirin crystals. *Chem. Eng. Res. Des.* **2018**, *132*, 170−177.
(52) Meier, M.; John, E.; Wieckhusen, D.; Wirth, W.; Peukert, W. Influence of mechanical properties on impact fracture: Prediction of the milling behaviour of pharmaceutical powders by nanoindentation. *Powder Technol.* **2009**, *188*, 301−313.
(53) Taylor, L. J.; Papadopoulos, D. G.; Dunn, P. J.; Bentham, A. C.; Dawson, N. J.; Mitchell, J. C.; Snowden, M. J. Predictive milling of pharmaceutical materials using nanoindentation of single crystals. *Org. Process Res. Dev.* **2004**, *8*, 674−679.
(54) Zugner, S.; Marquardt, K.; Zimmermann, I. Influence of nanomechanical crystal properties on the comminution process of particulate solids in spiral jet mills. *Eur. J. Pharm. Biopharm.* **2006**, *62*, 194−201.
(55) Mirtic, A.; Reynolds, G. K. Determination of breakage rate and breakage mode of roller compacted pharmaceutical materials. *Powder Technol.* **2016**, *298*, 99−105.
(56) Israelachvili, J. N. *Intermolecular and Surface Forces*, 3rd ed.; Elsevier Academic Press Inc: San Diego, 2011.
(57) Vainshtein, B. K. *Fundamentals of crystals: symmetry, and methods of structural crystallography*; Springer Science & Business Media, 2013; Vol. *1*.
(58) Mullin, J. W. *Crystallization*; Elsevier, 2001.
(59) Desiraju, G. R. Hydrogen bridges in crystal engineering: Interactions without borders. *Acc. Chem. Res.* **2002**, *35*, 565−573.
(60) Steiner, T. The hydrogen bond in the solid state. *Angew. Chem., Int. Ed.* **2002**, *41*, 48−76.
(61) Lawn, B. R. *Fracture of Brittle Solids*, 2nd ed.; Cambridge University Press: Cambridge, 1993.
(62) Perez, N. *Fracture Mechanics*, 2nd ed.; Springer Intl.: New York, 2017.
(63) de Vegt, O.; Vromans, H.; Pries, W.; Maarschalk, K. V. The effect of crystal imperfections on particle fracture behaviour. *Int. J. Pharm.* **2006**, *317*, 47−53.
(64) de Vegt, O.; Vromans, H.; den Toonder, J.; Maarschalk, K. v. d. V. Influence of flaws and crystal properties on particle fracture in a jet mill. *Powder Technol.* **2009**, *191*, 72−77.
(65) Anderson, P. M.; Hirth, J. P.; Lothe, J. *Theory of Dislocations*, 3rd ed.; Cambridge University Press: NY, 2017.
(66) Anslyn, E. V.; Dougherty, D. A. *Modern Physical Organic Chemistry*; University Science: Sausalito, CA, 2006.
(67) Dill, K. A.; Bromberg, S. *Molecular Driving Forces*, 2nd ed.; Garland Science: New York, 2011.
(68) Soga, N. Elastic-Moduli and Fracture-Toughness Of Glass. *J. Non-Cryst. Solids* **1985**, *73*, 305−313.
(69) Yuan, C. C.; Xi, X. K. On the correlation of Young's modulus and the fracture strength of metallic glasses. *J. Appl. Phys.* **2011**, 109.
(70) Gent, M.; Menendez, M.; Torano, J.; Torno, S. A correlation between Vickers Hardness indentation values and the Bond Work Index for the grinding of brittle minerals. *Powder Technol.* **2012**, *224*, 217−222.

https://dx.doi.org/10.1021/acs.joc.1c00121
J. Org. Chem. XXXX, XXX, XXX−XXX